PCCP

ROYAL SOCIETY OF CHEMISTRY

COMMUNICATION

View Article Online
View Journal | View Issue

Cite this: *Phys. Chem. Chem. Phys.*, 2025, **27**, 13812

Received 7th April 2025,
Accepted 11th June 2025

DOI: 10.1039/d5cp01321f

rsc.li/pccp

Magnetoresistance in Au/1,4-benzene-dithiol/Au and Au/1,4-benzene-dimethanethiol/Au single-molecule junctions†

Rachmat Andika,[a] Grace Gita Redhyka,[b] Ryo Yamada *[a] and Hirokazu Tada *[a]

Positive and negative magnetoresistance (MR) in single-molecule Au/BDT/Au and Au/BDMT/Au junctions appeared at 100 mT, revealing π-orbital influence. Differences in MR behaviors arise from singlet–triplet state modulation by exchange interaction, explaining the MR sign reversal. These findings provide new insight into magneto-transport in π-conjugated molecular junctions.

1. Introduction

Charge transport in single-molecule junctions has attracted considerable attention because it provides valuable insights into fundamental research in molecular electronics.[1] Various molecular responses to external stimuli have been utilized to create electronic functions.[1–3] For instance, photo-induced switching has been demonstrated through reversible isomerization between the open and closed forms of the diarylethene molecular structure.[4] Electrical current rectification has been achieved by modulating the energy levels[5] and orbital deformation[6] of asymmetric molecules.

The response of single-molecule junctions to magnetic fields, such as magnetoresistance (MR), has emerged as an increasingly significant area of research.[7] Ferromagnetic electrodes are typically used to observe MR.[8–10] However, MR has also been reported in single molecular junctions with non-magnetic gold (Au) electrodes,[11,12] suggesting that MR can arise from molecular properties. Hayakawa *et al.* observed an increase in electrical resistance (positive MR) under a magnetic field of 4 T at 4.2 K in single-molecule junctions of oligo (*p*-phenylene ethynylene) with Au electrodes.[11] They proposed that the magnetic field reduces the electronic coupling between the π-orbital and the electrodes, leading to positive MR. Similarly, Mitra *et al.* observed both negative and positive MR in single-molecule junctions of perchlorotrityl-derived molecules under a 6 T magnetic field at 4.2 K.[12] They attributed these MR effects to a change in electron scattering at the interface between the π-conjugated molecule and the Au electrode.

Xie *et al.* reported a positive MR of up to 38% in a self-assembled monolayer (SAM) of oligophenylene (OPE)-thiol molecule at room temperature.[13] They attributed this effect to the strong dipole moment at the Au/S interface. Shi *et al.* proposed a mechanism based on the singlet (S) and triplet (T) states.[14] This S–T mechanism is applicable for non-radical molecules by assuming the injection of an electron at the Au/S interface. Specifically, the spin coupling between the unpaired charge in the molecular orbital (MO) and the transporting electrons creates S and T states at the interface, acting as transport channels and altering electrical resistance in response to the magnetic field. In the absence of a magnetic field and when the energy gap between S and T states is small, all states contribute to the charge transport. Under a magnetic field, the T states split, reducing their contribution to transmission and increasing resistance (positive MR). Their theoretical analysis also revealed the emergence of negative MR, which they linked to charge injection into the π-orbital as the cause of the MR effect.

In this work, we observed both positive and negative MR for single-molecule junctions based on 1,4-benzene-dithiol (BDT) and 1,4-benzene-dimethanethiol (BDMT) with Au electrodes, under a magnetic field of 100 mT at room temperature. Positive MR was more frequently observed than negative MR in both junctions and occurred more often in Au/BDMT/Au junctions than in Au/BDT/Au junctions. We discuss the mechanism underlying the occurrence of negative MR in this system.

2. Electrical conductance of molecular junctions

2.1. Mechanically controllable break junction (MCBJ) method

Before MR measurements, the electrical conductance (G) of Au/BDT/Au and Au/BDMT/Au junctions was determined. The

[a] *Graduate School of Engineering Science, Osaka University, Machikaneyama 1-3, Toyonaka, Osaka, 5608531, Japan. E-mail: tada.hirokazu.es@osaka-u.ac.jp*
[b] *Research Center for Quantum Physics, National Research and Innovation Agency (BRIN), Tangerang Selatan, 15314, Indonesia*

† Electronic supplementary information (ESI) available. See DOI: https://doi.org/10.1039/d5cp01321f

electrical conductance of single-molecule junctions was measured at room temperature using the mechanically controllable break junction (MCBJ) method.[10] Fig. 1 depicts the MCBJ setup along with the molecular structures of Au/BDT/Au and Au/BDMT/Au junctions.

The details of the MCBJ method have been described elsewhere.[15] In brief, the MCBJ method employs a three-point bending mechanism consisting of a pushing rod beneath the substrate and two support beams on either side. A suspended gold (Au) nano-contact was fabricated *via* electrodeposition on an elastic substrate composed of a polyimide layer on a phosphorus bronze sheet, as shown in Fig. 1.[16,17] After mounting the substrate onto the three-point bending mechanism, a drop of 1 mM molecular solution in ethanol was applied to the Au contact to functionalize the Au electrode with molecules. The excess solution was removed by drying with argon (Ar) gas.

Measurements began by raising the pushing rod to bend the substrate. As the substrate bent, the Au nano-contact elongated and eventually formed an Au atomic contact. Just before the complete rupture of the Au atomic contact, one or more molecules could bridge the gap between electrodes, creating single-molecule junctions. The breaking and re-forming of the Au contact, *i.e.*, the creation of single-molecule junctions, could be repeated by adjusting the position of the pushing rod.

During the breaking process, electrical conductance (G) was monitored to analyze the structure of the junction, as represented by conductance traces (G-traces). A single Au atomic junction typically exhibits a conductance plateau at $G = 1G_0$ where $G_0 = 2e^2/h \approx 7.75 \times 10^{-5}$ S (e is the elementary charge of the electron and h is the Planck's constant). Single-molecule junctions display conductance plateaus at $G < 1\ G_0$, with variations due to differences in contact geometry.[18,19]

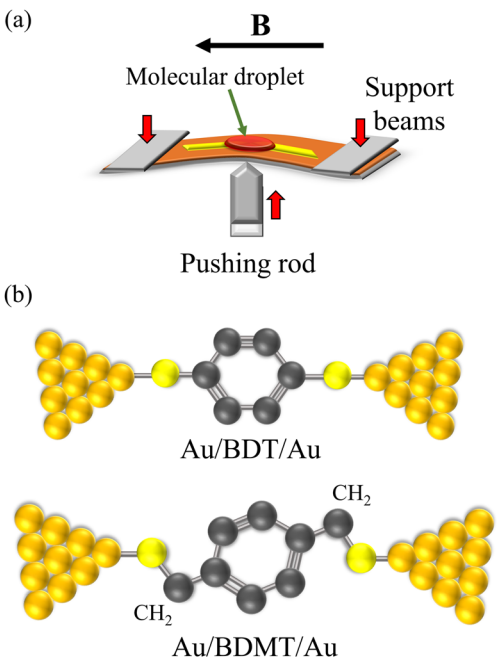

Fig. 1 Illustration of (a) MCBJ setup and (b) single-molecule junctions of BDT and BDMT molecules. For simplicity, the hydrogen (H) atoms were omitted in the figure. In Au/BDMT/Au junctions, the phenyl ring and Au/S interfaces are separated by a methylene ($-CH_2$) unit.

2.2. Results and discussion

Fig. 2(a) presents the G-histogram constructed from 106 G-traces at a bias voltage (V_B) of 30 mV, with a typical G-trace shown in the inset. The plateaus at different G values indicate the formation of multiple stable junction structures, resulting from various molecular conformations and contact geometries.[20,21] Gaussian curve fitting reveals two prominent maxima at $G = 3.2 \times 10^{-2}\ G_0$ and $3.2 \times 10^{-4}\ G_0$ which correspond to single-molecule junctions with bridge and on-top configurations, respectively.[22] Fig. 2(b) displays the G-histogram constructed from 140 G-traces and a typical G-trace (inset) for BDMT molecules on the Au electrode at $V_B = 30$ mV. Two distinct peaks are observed at $G = 1.6 \times 10^{-1}\ G_0$ and $G = 2.5 \times 10^{-3}\ G_0$, closely matching the values reported by Xiao *et al.*[23]

3. Magnetoresistance (MR) measurement

3.1. Experimental method

We employed the MCBJ method with an external magnetic field applied using an electromagnet.[10] For MR measurements, single-molecule junctions are needed to remain stable for several seconds to allow the magnetic field sweep. Since most junctions broke within a second, MR measurements were conducted only on stable junctions lasting at least one second. The magnetic field (B) was swept from −100 mT to +100 mT at a rate of 40 mT s^{-1} aligned parallel to the current flow. The time-series data of the magnetic field and resistance are provided in Fig. S2 of the ESI.† The MR curve presented was reproducible in the forward-backward sweep. No significant difference in MR was observed when the magnetic field was applied perpendicular to the current flow. The resistance (R) was calculated as $R = 1/G$, where G is the conductance. The MR percentage was defined as:

$$\mathrm{MR} = \frac{(R_B - R_0)}{R_0} \times 100\%$$

where R_0 is the resistance at $B = 0$ T and R_B is the resistance value at $B \neq 0$ T.

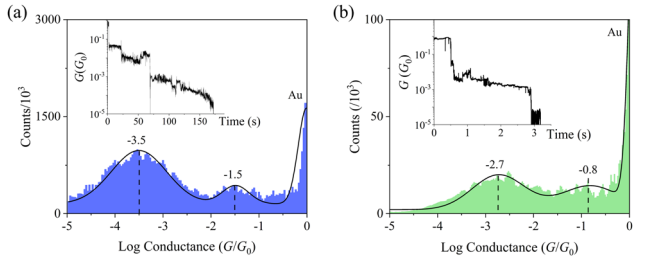

Fig. 2 G-histograms and the representative of G-traces (insets) for (a) Au/BDT/Au and (b) Au/BDMT/Au junctions.

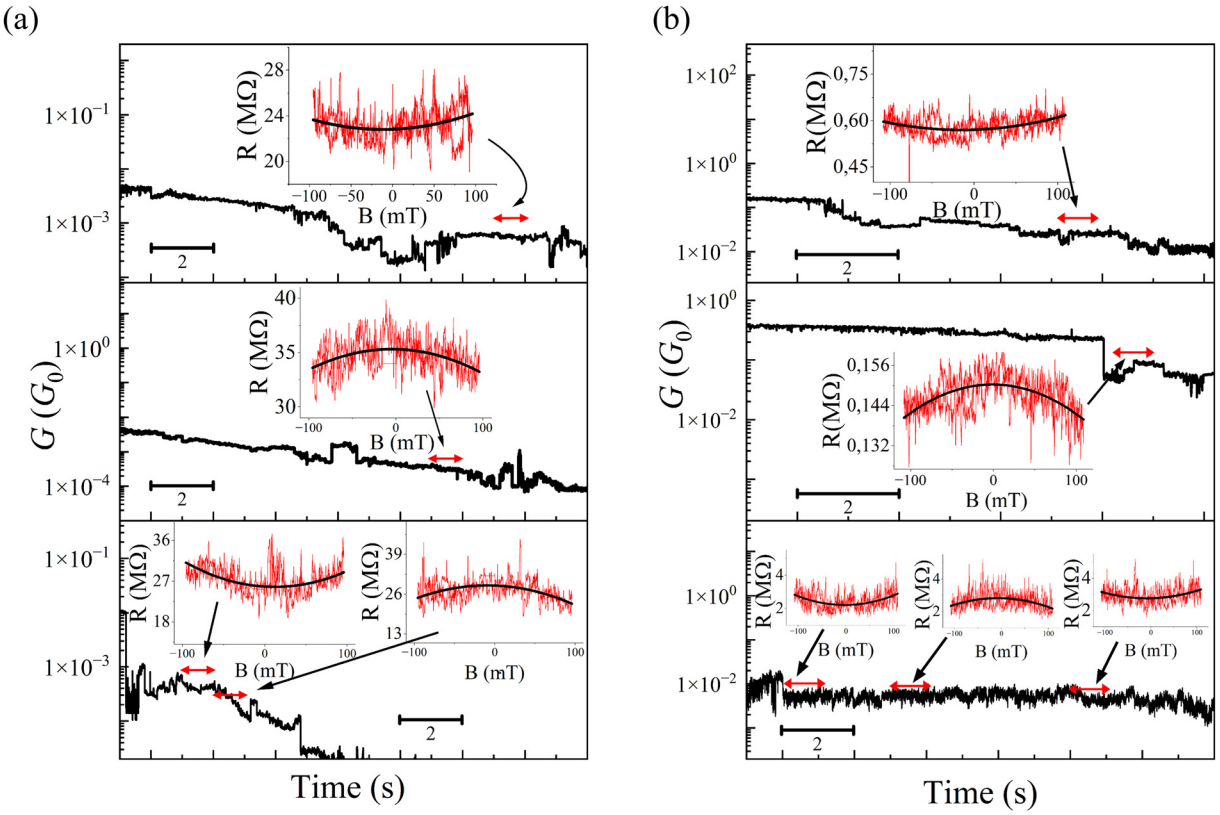

Fig. 3 Various individual *G*-traces for (a) Au/BDT/Au and (b) Au/BDMT/Au junctions, with the MR curves fitted by a parabolic function shown in the insets. Red arrows indicate the periods of the MR measurements. Scale bars represent the time scale, in seconds, during the breaking process.

3.1. Results and discussion

Fig. 3 presents typical *G*-traces for (b) Au/BDT/Au and (c) Au/BDMT/Au junctions with their corresponding MR behaviors (insets). The data were processed using the Savitzky–Golay smoothing filter to reduce signal noise[24] (see ESI† for a comparison of raw and processed data). The MR curves were fitted using parabolic functions (solid black line) as a visual guide, aiding in the MR ratio estimation while minimizing the effect of noise.

Fig. 4 summarizes the histogram of the estimated MR percentage for the MR curves obtained from Au/BDT/Au and Au/BDMT/Au single-molecule junctions. For Au/BDT/Au, 14 MR curves were identified out of 1500 measurements—7 positive and 7 negative—MR curves resulting in an appearance ratio of 1 : 1. For Au/BDMT/Au, 19 MR curves were observed, comprising 13 positive and 6 negative MR curves, yielding an appearance ratio of approximately 2 : 1. The average positive MR percentages were +18% for Au/BDT/Au and +13% for Au/BDMT/Au/junctions. The average negative MR percentages were −13% and −9%, respectively. The MR sign was observed to change during the *G*-measurement process, as shown in the inset of Fig. 3, suggesting that the MR is highly sensitive to the junction structures.[25,26] The different conductance values are frequently associated with the various contact geometries.[18] However, the MR found in this study showed that the contact geometries have no strong influence on the MR.

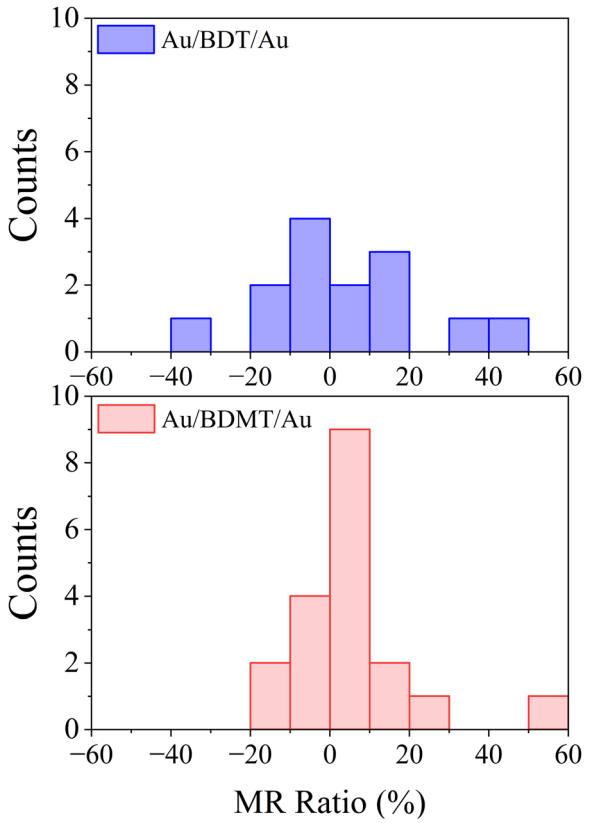

Fig. 4 Histogram of MR percentage for Au/BDT/Au and Au/BDMT/Au single-molecule junction.

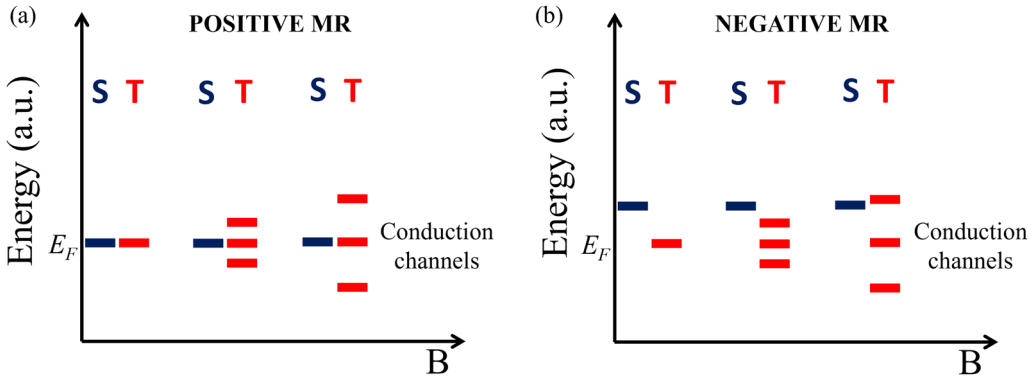

Fig. 5 The scheme of the MR mechanism for the (a) positive MR and (b) negative MR based on S–T states.[14] Due to exchange energy, the elevated initial T states in (b) created more conduction channels as the magnetic field was applied.

Our observation of negative MR contrasts with previous findings that reported only positive MR for non-π-conjugated molecules, such as 1,6-hexanedithiol, inserted between Au electrodes.[27] This discrepancy suggests that the π orbital plays a crucial role in exhibiting negative MR by modifying the electronic state at the Au/S interface. Earlier reports support this claim, emphasizing the influence of the π orbital on the Au/S interface in *para*-BDMT molecules between Au nanogaps.[28] The presence of a methylene ($-CH_2$) unit in BDMT weakens electronic coupling between the Au/S interface and the π-orbital, increasing the likelihood of positive MR. Furthermore, negative MR was observed less frequently than positive MR, indicating that the Au–S–π configuration associated with the negative MR is rarely achieved. This likely explains why only positive MR was observed in the SAM films.[13]

Additionally, Ghosh *et al.* found that the π-orbital enhances the energy gap between singlet (S) and triplet (T), further underscoring the significant role of the π-orbital in molecular junctions[29] Based on these findings, the negative MR can be explained by the S–T mechanism proposed by Shi.[14] Fig. 5(a) and (b) illustrate the potential mechanisms for positive and negative MR, respectively. For simplicity, energy level broadening is not considered.

When the S and T states are close to the Fermi energy (E_F), splitting the T states under a magnetic field reduces the total transmission due to decreased contribution from the T states, resulting in positive MR. Conversely, when an energy gap exists between the S and the T states, splitting the T states enhances transmission as the split T state shifts closer to E_F, leading to negative MR.

The MR sign change observed in Fig. 4 may depend on the extent to which an exchange interaction elevates the S state, where variations in exchange interaction produce different exchange magnetic fields (B_{exc}). This B_{exc} governs the MR sign change. When B_{exc} exceeds 100 mT, negative MR emerges, while for B_{exc} below 100 mT or in the absence of exchange interaction ($B_{exc} = 0$), positive MR dominates. Our findings support the S–T theoretical model proposed by Shi *et al.*[14] and provide valuable insights into MR in single-molecule junctions without requiring ferromagnetic electrodes.

4. Conclusion

Using the MCBJ method, we observed both positive and negative MR in Au/BDT/Au and Au/BDMT/Au single-molecule junctions. Our findings indicate that positive MR results from energy level shifts in the S and T states at the Au/S interface, driven by the hybridization between the π-orbital and the electronic state of the Au electrode. In contrast, negative MR stems from changes in the relationship between the S and T states due to the variations in electronic coupling of the π orbital. The presence of the methylene group in BDMT may weaken this coupling, increasing the likelihood of positive MR. These results provide valuable insights into MR mechanisms in single-molecule junctions and emphasize the critical role of π orbitals in influencing MR behavior.

Author contributions

RA: conceptualization, conducting a research and investigation process, specifically performing the experiments, or data/evidence collection, writing original draft, writing – review & editing; GGR: conceptualization, review – editing; RY: conceptualization, formal analysis, writing – review & editing; HT: conceptualization, writing – review & editing, supervision.

Conflicts of interest

There are no conflicts to declare.

Data availability

All data supporting the findings of this study, including those presented in the main text and ESI.†

Acknowledgements

This work was financially supported by JSPS KAKENHI Grant Number 22H00315 and 18H03899. RA thanks JICA (Japan International Cooperation Agency) for the scholarship during

the research period. RA acknowledges Yusuf Wicaksono, PhD, NIMS, for the fruitful discussions during the research period.

References

1 H. Zhang, J. Li, C. Yang and X. Guo, Single-molecule functional chips: unveiling the full potential of molecular electronics and optoelectronics, *Acc. Mater. Res.*, 2024, **5**, 971–986.
2 N. Xin, J. Guan, C. Zhou, X. Chen, C. Gu, Y. Li, M. A. Ratner, A. Nitzan, J. F. Stoddart and X. Guo, Concepts in the design and engineering of single-molecule electronic devices, *Nat. Rev. Phys.*, 2019, **1**, 211–230.
3 Q. Zou, J. Qiu, Y. Zang, H. Tian and L. Venkataraman, Modulating single-molecule charge transport through external stimulus, *eScience*, 2023, **3**, 100115.
4 C. Jia, A. Migliore, N. Xin, S. Huang, J. Wang, Q. Yang, S. Wang, H. Chen, D. Wang, B. Feng, Z. Liu, G. Zhang, D.-H. Qu, H. Tian, M. A. Ratner, H. Q. Xu, A. Nitzan and X. Guo, Covalently bonded single-molecule junctions with stable and reversible photoswitched conductivity, *Science*, 1979, **2016**(352), 1443–1445.
5 M. Handayani, H. Tanaka, S. Katayose, T. Ohto, Z. Chen, R. Yamada, H. Tada and T. Ogawa, Three site molecular orbital controlled single-molecule rectifiers based on perpendicularly linked porphyrin-imide dyads, *Nanoscale*, 2019, **11**, 22724–22729.
6 R. Yamada, K. Albrecht, T. Ohto, K. Minode, K. Yamamoto and H. Tada, Single-molecule rectifiers based on voltage-dependent deformation of molecular orbitals in carbazole oligomers, *Nanoscale*, 2018, **10**, 19818–19824.
7 H. Gu, X. Zhang, H. Wei, Y. Huang, S. Wei and Z. Guo, An overview of the magnetoresistance phenomenon in molecular systems, *Chem. Soc. Rev.*, 2013, **42**, 5907–5943.
8 K. Horiguchi, T. Sagisaka, S. Kurokawa and A. Sakai, Electron transport through Ni/1,4-benzenedithiol/Ni single-molecule junctions under magnetic field, *J. Appl. Phys.*, 2013, **113**(14), 144313.
9 K. Yoshida, I. Hamada, S. Sakata, A. Umeno, M. Tsukada and K. Hirakawa, Gate-Tunable large negative tunnel magnetoresistance in Ni–C 60 –Ni single molecule transistors, *Nano Lett.*, 2013, **13**, 481–485.
10 R. Yamada, M. Noguchi and H. Tada, Magnetoresistance of single molecular junctions measured by a mechanically controllable break junction method, *Appl. Phys. Lett.*, 2011, **98**, 053110.
11 R. Hayakawa, M. A. Karimi, J. Wolf, T. Huhn, M. S. Zöllner, C. Herrmann and E. Scheer, Large magnetoresistance in single-radical molecular junctions, *Nano Lett.*, 2016, **16**, 4960–4967.
12 G. Mitra, J. Z. Low, S. Wei, K. R. Francisco, M. Deffner, C. Herrmann, L. M. Campos and E. Scheer, Interplay between Magnetoresistance and kondo resonance in radical single-molecule junctions, *Nano Lett.*, 2022, **22**, 5773–5779.
13 Z. Xie, S. Shi, F. Liu, D. L. Smith, P. P. Ruden and C. D. Frisbie, Large magnetoresistance at room temperature in organic molecular tunnel junctions with nonmagnetic electrodes, *ACS Nano*, 2016, **10**, 8571–8577.
14 S. Shi, Z. Xie, F. Liu, D. L. Smith, C. D. Frisbie and P. P. Ruden, Theory of magnetoresistance of organic molecular tunnel junctions with nonmagnetic electrodes, *Phys. Rev. B*, 2017, **95**, 1–9.
15 L. Wang, L. Wang, L. Zhang and D. Xiang, Advance of Mechanically Controllable Break Junction For Molecular Electronics, *Top. Curr. Chem.*, 2017, **375**(3), 61.
16 A. K. Mahapatro, S. Ghosh and D. B. Janes, Nanometer scale electrode separation (nanogap) using electromigration at room temperature, *IEEE Trans. Nanotechnol.*, 2006, **5**, 232–236.
17 J.-H. Tian, Y. Yang, B. Liu, B. Schöllhorn, D.-Y. Wu, E. Maisonhaute, A. S. Muns, Y. Chen, C. Amatore, N.-J. Tao and Z.-Q. Tian, The fabrication and characterization of adjustable nanogaps between gold electrodes on chip for electrical measurement of single molecules, *Nanotechnology*, 2010, **21**, 274012.
18 K.-R. Chiang and Y.-H. Tang, Effect of Contact Geometry on Spin Transport in Amine-Ended Single-Molecule Magnetic Junctions, *ACS Omega*, 2021, **6**, 19386–19391.
19 X. Li, J. He, J. Hihath, B. Xu, S. M. Lindsay and N. Tao, Conductance of single alkanedithiols: Conduction mechanism and effect of molecule-electrode contacts, *J. Am. Chem. Soc.*, 2006, **128**, 2135–2141.
20 J. Hihath and N. Tao, The role of molecule–electrode contact in single-molecule electronics, *Semicond. Sci. Technol.*, 2014, **29**, 054007.
21 M. Gil, T. Malinowski, M. Iazykov and H. R. Klein, Estimating single molecule conductance from spontaneous evolution of a molecular contact, *J. Appl. Phys.*, 2018, **123**, 104303.
22 Y. Komoto, S. Fujii, H. Nakamura, T. Tada, T. Nishino and M. Kiguchi, Resolving metal-molecule interfaces at single-molecule junctions, *Sci. Rep.*, 2016, **6**, 1–9.
23 X. Xiao, B. Xu and N. J. Tao, Measurement of single molecule conductance: benzenedithiol and benzenedimethanethiol, *Nano Lett.*, 2004, **4**, 267–271.
24 R. W. Schafer, What is a savitzky-golay filter?, *IEEE Signal Process. Mag.*, 2011, **28**, 111–117.
25 S. Kobayashi, S. Kaneko, M. Kiguchi, K. Tsukagoshi and T. Nishino, Tolerance to stretching in thiol-terminated single-molecule junctions characterized by surface-enhanced Raman scattering, *J. Phys. Chem. Lett.*, 2020, **11**, 6712–6717.
26 L. Venkataraman, J. E. Klare, C. Nuckolls, M. S. Hybertsen and M. L. Steigerwald, Dependence of single-molecule junction conductance on molecular conformation, *Nature*, 2006, **442**, 904–907.
27 R. Andika, R. Yamada and H. Tada, Magnetoresistance originated from the Au/S interface in Au/1,6-hexanedithiol/Au single-molecule junctions at room temperature, *Phys. Chem. Chem. Phys.*, 2023, **25**, 18642–18645.
28 S. Guan, Z. Cai, J. Liu, R. Pang, D. Wu, J. Ulstrup and Z. Tian, Adsorption, stretching, and breaking processes in single-molecule conductance of *para*-Benzenedimethanethiol in gold nanogaps: a DFT-NEGF theoretical study, *ChemElectroChem*, 2021, **8**, 1123–1133.
29 R. Ghosh, P. Seal and S. Chakrabarti, Role of π-conjugation in influencing the magnetic interactions in dinitrenes: a broken-symmetry approach, *J. Phys. Chem. A*, 2010, **114**, 93–96.